Structural differences determine the relative selectivity of nicotinic compounds for native α4β2*-, α6β2*-, α3β4*- and α7-nicotine acetylcholine receptors

Sharon R. Grady [a,*], Ryan M. Drenan [b], Scott R. Breining [c], Daniel Yohannes [c], Charles R. Wageman [a], Nikolai B. Fedorov [c], Sheri McKinney [b], Paul Whiteaker [a,1], Merouane Bencherif [c], Henry A. Lester [b], Michael J. Marks [a]

[a] Institute for Behavioral Genetics, University of Colorado, Boulder, CO 80309, USA
[b] Division of Biology, California Institute of Technology, Pasadena, CA 91125, USA
[c] Department of Preclinical Research, Targacept Inc., Winston-Salem, NC 27101, USA

ARTICLE INFO

ABSTRACT

Mammalian brain expresses multiple nicotinic acetylcholine receptor (nAChR) subtypes that differ in subunit composition, sites of expression and pharmacological and functional properties. Among known subtypes of receptors, α4β2* and α6β2*-nAChR have the highest affinity for nicotine (where * indicates possibility of other subunits). The α4β2*-nAChRs are widely distributed, while α6β2*-nAChR are restricted to a few regions. Both subtypes modulate release of dopamine from the dopaminergic neurons of the mesoaccumbens pathway thought to be essential for reward and addiction. α4β2*-nAChR also modulate GABA release in these areas.

Identification of selective compounds would facilitate study of nAChR subtypes. An improved understanding of the role of nAChR subtypes may help in developing more effective smoking cessation aids with fewer side effects than current therapeutics. We have screened a series of nicotinic compounds that vary in the distance between the pyridine and the cationic center, in steric bulk, and in flexibility of the molecule. These compounds were screened using membrane binding and synaptosomal function assays, or recordings from GH4C1 cells expressing hα7, to determine affinity, potency and efficacy at four subtypes of nAChRs found in brain, α4β2*, α6β2*, α7 and α3β4*. In addition, physiological assays in gain-of-function mutant mice were used to assess in vivo activity at α4β2* and α6β2*-nAChRs. This approach has identified several compounds with agonist or partial agonist activity that display improved selectivity for α6β2*-nAChR.

© 2010 Elsevier Ltd. All rights reserved.

1. Introduction

Dependence on nicotine partially underlies the difficulty encountered in smoking cessation. Currently available smoking cessation aids (nicotine replacement, bupropion or varenicline treatment) are helpful for a subset of the population, with variable relapse prevention (Lerman et al., 2007; De Biasi and Salas, 2008). There is a need for treatments with improved effectiveness, relapse prevention, tolerability, and safety.

Nicotine elicits physiological and behavioral effects through actions as an agonist and/or desensitizer at nicotinic acetylcholine receptors (nAChRs). nAChRs in brain exist as pentamers made up of the α2-7, and β2-4 subunits. Some nAChRs are homomers (α7), but most are heteromers (β2 or β4 in combination with α subunits)

(Gotti et al., 2006). α4β2*-nAChRs, which comprise the most widely expressed high-affinity subtypes, play a major role in modulating the effects of smoked nicotine (Mameli-Engvall et al., 2006; Keath et al., 2007). Some α4β2*-nAChRs are upregulated by chronic exposure to nicotine (Flores et al., 1992; McCallum et al., 2006; Nashmi et al., 2007; Lester et al., 2009).

The α4α6β3β2 nAChR has the highest sensitivity for nicotine of any subtypes studied to date (Salminen et al., 2007). In contrast to the widespread distribution of α4β2*-nAChR, α6β2*-nAChRs have a restricted distribution, localized primarily to dopamine (DA) neurons, noradrenergic neurons, and visual tracts (Whiteaker et al., 2000b; Champtiaux et al., 2002, 2003; Quik et al., 2003; Drenan et al., 2008). Both of these β2*-nAChR subtypes are important regulators of DA release in the nucleus accumbens, which participates in the rewarding effects of nicotine (Exley et al., 2008). α6β2*-nAChRs in mesoaccumbens dopaminergic neurons may be necessary for nicotine self-administration (Pons et al., 2008). Interestingly, α6β2*-nAChRs, despite their high sensitivity to nicotine, are upregulated at comparatively high nicotine concentrations when expressed in HEK

---

* Corresponding author. Tel.: +1 303 492 9677; fax: +1 303 492 8063.
E-mail address: sharon.grady@colorado.edu (S.R. Grady).
[1] Present address: Barrow Neurological Institute, St. Joseph's Hospital and Medical Center, Phoenix, AZ 85013, USA.

cells (Tumkosit et al., 2006), while they are downregulated following chronic nicotine treatment in rats and mice (Lai et al., 2005; Perry et al., 2007; Perez et al., 2008).

Whole genome scans in humans have detected genetic associations between α6-nAChR subunit genes and aspects of human smoking. The CHRNA6/B3 gene cluster has significant associations with subjective responses to nicotine (Zeiger et al., 2008), tobacco dependence, and number of quit attempts (Hoft et al., 2008). These associations may suggest that α6*-nAChRs could be an important target for nicotine. nAChR subtype selective compounds will become pharmacological tools to help identify how various subtypes affect the acquisition and maintenance of addiction, as well as which subtypes are good targets for smoking cessation therapy. Selective compounds may enable therapies to be tailored to individuals by combining genetic association data with appropriate smoking cessation aids (Ho and Tyndale, 2007).

Based on knowledge gained using nAChR subunit null mutant mice and various selective agonists and antagonists, we have devised a battery of assays to assess binding affinity, functional potency and efficacy at four subtypes of nAChR (α4β2*, α6β2*, α7 and α3β4*). Gain-of-function α4L9′A (Tapper et al., 2007) and α6L9′S (Drenan et al., 2008) mice have been developed to evaluate selective activation of α4β2* or α6β2*-nAChR in vivo. We have assessed the effects of structural modifications of nicotine that may improve selectivity for α4β2* and/or α6β2*-nAChRs.

2. Methods

2.1. Materials

[125I]-α-bungarotoxin (α-Btx, specific activity 2000 Ci/mmol) was a product of GE Healthcare, Little Chalfont, Buckinghamshire, UK. [125I]-epibatidine (2200 Ci/mmol), [3H]dopamine (3,4-[ring-2,5,6-3H], 30–60 Ci/mmol), [3H]choline (methyl-3H, 60–90 Ci/mmol), and carrier-free 86RbCl were purchased from Perkin Elmer Life Sciences, Boston, MA. α-Conotoxin MII (α-CtxMII) and [125I]-α-CtxMII were obtained from J. Michael McIntosh, University of Utah, Salt Lake City, UT. The following chemicals as well as all buffer components (Reagent Grade) were products of Sigma−Aldrich (St Louis, MO): A-85380, atropine, aprotinin, bovine serum albumin (BSA), α-cobratoxin, EDTA, EGTA, (±)-epibatidine, HEPES, (−)-nicotine tartrate, leupeptin, nomifensine, pargyline, pepstatin A, PMSF, polyethylenimine and tetrodotoxin.

2.2. Compound synthesis

Compounds 1 (RJR2429, TC2429, (±)-2-(-3-pyridinyl)-1-azabicyclo[2.2.2] octane), 3 (TC1698, 2-(pyridine-3-yl)-1-azabicyclo[3.2.2]nonane), 6 (TC6951, (4S)-2-(5-phenylpyridin-3-yl)quinuclidine) and 7 (TC2242, 4-(5-(quinuclidin-2-yl)pyridin-3-yloxy)benzonitrile) were synthesized using previously published methods (Bhatti et al., 2008 compounds 3, 6, 26, and 29, respectively). Varenicline was synthesized by the methods of Coe et al. (2005) and Compound 8 (RJR2403, TC2403, (E)-N-methyl-4-(3-pyridinyl)-3-butene-1-amine) following the methods of Bencherif et al. (1996). For other compounds: Compound 2: (7-(pyridin-3-yl)-1-azabicyclo[2.2.1]heptane) Bencherif, Merouane; Miller, Craig Harrison; Hawkins, Gregory D.; Bhatti, Balwinder S., preparation of pyridinyl substituted azabicyclic compounds for use in pharmaceutical compositions which effect dopamine release, U.S. Pat. Appl. US2004220214. Compound 4: (1-aza-2-(3-pyridinyl)-tricyclo[3.3.1.13,7]decane) Bencherif, Merouane; Lippiello, Patrick Michael; Crooks, Peter Anthony; Park, Haeil; Bhatti, Balwinder Singh; Caldwell, William Scott; Dull, Gary Maurice, preparation of azatricyclo [3.3.1.13,7]decanes and related compounds as nicotinic antagonists, PCT Int. Appl. WO9951602.Compound 5: (2-(pyridin-3-ylmethyl)quinuclidine) Schmitt, Jeffrey Daniel; Crooks, Peter Anthony; Dull, Gary Maurice, preparation of pyridyl-bridgehead derivatives and their analogs, pharmaceutical compositions and methods for use, US Patent 6,432,975. Compound 9: ((E)-N-methyl-5-(5-(phenylethynyl)pyridin-3-yl)pent-4-en-2-amine) was prepared from known 3-bromo-5-(2-phenylethynyl)-pyridine (Agejas-Chicharro, Francisco Javier; Dressman, Bruce Anthony; Gutierrez Sanfeliciano, Sonia; Henry, Steven Scott; Martinez Perez, Jose Antonio; Massey, Steven Marc; Monn, James Allen; Zia-Ebrahimi, Mohammad Sadegh, preparation of pyridines as mGlu5 receptor antagonists, PCT Int. Appl. WO2005094822), according to the general methods cited in: Caldwell, William Scott; Dull, Gary Maurice; Dobson, Grayland, 3-pyridinyl compounds. US 6,603,011. Compound 10: ((1R,5S)-3-(5-bromopyridin-3-yl)-8-methyl-8-azabicyclo[3.2.1]oct-3-ene) was prepared analogously to compounds reported previously (Gohlke et al., 2003). Compound 11 (2-((5-chloropyridin-3-yloxy)methyl)quinuclidine) was prepared as described previously (Zhao et al., 2002).

2.3. Animals

All animal procedures were in accordance with the guidelines of the National Institutes of Health. Mice of the C57BL/6J strain 60–90 days of age, used for this study were bred and maintained at the Institute for Behavioral Genetics, University of Colorado, Boulder, CO. After weaning at 25 days of age, same sex littermates were housed 5 to a cage with free access to food (Teklad Rodent Diet, Harlan, Madison, WI) and water, with a 12-h light/dark cycle at 22 °C. Mice of the α4 subunit null mutant mice (originally from Dr. John Drago), were bred and maintained as above and genotyped as previously described (Salminen et al., 2004). Animal care and experimental procedures for these mice were in accordance with the guidelines and approval of the Animal Care and Utilization Committee of the University of Colorado, Boulder, CO.

Hypersensitive α4L9′A knock-in mice (Tapper et al., 2007) and α6L9′S (Drenan et al., 2008) transgenic mice were bred and maintained at the California Institute of Technology, Pasadena, CA. Animal care and experimental procedures with these mice were approved by the California Institute of Technology Animal Care and Use Committee.

2.4. Tissue preparation for binding studies

The methods of Marks et al. (1998, 2006) were followed for preparation of brain membranes in hypotonic buffer. These membrane preparations were stored as pellets under buffer at −70 °C or used immediately for [125I]-α-Btx and [125I]-epibatidine binding. The method of Salminen et al. (2005) was used for [125I]-α-CtxMII binding. Briefly, regions high in α-CtxMII binding sites (olfactory tubercles (OT), striatum (ST) and superior colliculus (SC)) were pooled and homogenized in hypertonic (2×) buffer (NaCl, 288 mM; KCl, 3 mM; CaCl2, 4 mM; MgSO4, 2 mM; HEPES, 40 mM; pH = 7.5) and then incubated with PMSF (1 mM) at 22 °C for 15 min to inactivate serine proteases. After centrifugation (20,000 × g for 15 min at 4 °C), the pellet was resuspended in hypotonic buffer and re-centrifuged twice. The final pellet was resuspended in distilled water and used without freezing.

2.5. [125I]-α-Bungarotoxin binding

A modification of previously published methods was used (Marks et al., 1998). Hippocampal homogenate samples (∼50 µg protein) were incubated with 1 nM [125I]-α-Btx in 30 µl binding buffer (NaCl, 144 mM; KCl, 1.5 mM; CaCl2, 2 mM; MgSO4, 1 mM; HEPES, 25 mM; pH 7.5) supplemented with 0.1% BSA in 96-well plates modified to hold 1 ml capacity tubes. Various concentrations of a compound to be tested for inhibition of [125I]-α-Btx binding were added to triplicate wells; non-specific binding was determined from wells to which α-cobratoxin (100 nM) was added. After incubation for 2.5 h at room temperature, samples were diluted with 0.5 ml binding buffer and incubated an additional 0.5 h. This dilution step decreases non-specific binding. Reaction was terminated by filtration onto glass fiber filters (MFS GB top layer, Gelman A/E bottom layer, both soaked in binding buffer containing 0.5% polyethylenimine) using an Inotech Cell Harvester (Inotech, Rockville, MD). Samples were washed 6 times with ice-cold binding buffer and bound [125I]-α-Btx was determined by counting at 60% efficiency in a 1450 MicroBeta Trilux scintillation counter after addition of Optiphase SuperMix scintillation cocktail (150 µl/sample) (Perkin Elmer Life Sciences-Wallac Oy, Turku, Finland).

2.6. [125I]-epibatidine binding

[125I]-epibatidine binding was determined using methods previously described (Marks et al., 1998; Whiteaker et al., 2000a) with minor modifications. As for [125I]-α-Btx binding various concentrations of a compound to be tested for inhibition of were added to triplicate wells. Briefly, for measurement of inhibition of [125I]-epibatidine binding (corresponding to binding to α4β2* sites) 100 pM [125I]-epibatidine was incubated with cortical membrane in 30 µl of binding buffer for 2 h at room temperature and then filtered onto a single thickness of polyethylenimine − soaked GFA/E glass fiber filter (Gelman Sciences, Ann Arbor, MI) and washed as for [125I]-α-Btx binding. For determining A85380-resistant [125I]-epibatidine binding (corresponding to binding to α3β4* sites), membranes prepared from interpeduncular nucleus (IPN) were assayed by including 10 nM A85380 (Sigma Chemical Co, St Louis, MO) with 200 pM [125I]-epibatidine. For both procedures, 1 mM (−)-nicotine tartrate was used to determine non-specific binding. Radioactivity was determined as for [125I]-α-Btx binding.

2.7. [125I]-α-CtxMII binding

The methods of Salminen et al. (2005, 2007) were followed. Membrane samples (40–50 µg protein) from pooled olfactory tubercle, striatum and superior colliculus were incubated with 0.5 nM [125I]-α-CtxMII in 30 µl binding buffer supplemented with BSA (0.1%), EDTA (5 mM), EGTA (5 mM), and the protease inhibitors, aprotinin, leupeptin and pepstatin A (10 µg/ml each). Various concentrations of a compound to be tested for inhibition were added to triplicate wells. Non-specific binding was determined from wells to which 1 nM epibatidine was added. Binding reactions were incubated at 22 °C for 2 h, then diluted with 1 ml of buffer containing 0.1% BSA and incubated 4 min longer. Reactions were terminated by filtration onto a single sheet of GF/F filter paper (Whatman, Clifton, NJ) treated with 5% nonfat dry milk for

30 min. Samples were washed four times with ice-cold buffer containing BSA (0.1%). Bound ligand was determined by beta counting as above. It has been demonstrated that this concentration of α-CtxMII measures α6*-nAChR in mouse dopaminergic and visual tractregions as no binding remains there in the α6 null mutant mouse (Champtiaux et al., 2002), and, in addition, the α3 null mutation has no effect on α-CtxMII binding in these regions (Whiteaker et al., 2002).

2.8. Membrane binding data analysis

After subtraction of non-specific binding, inhibition of binding was analyzed by using a one-site fit to the inhibition equation ($B = B_0/(1 + ([I]/IC_{50})$) where B is ligand bound in the presence of inhibitor at concentration [I], B_0 is ligand bound in the absence of inhibitor (Whiteaker et al., 2000a). K_i values were calculated from IC_{50} values using the equation ($K_i = IC_{50}/(1 + (L/K_D))$). Means ± sem from three to four experiments are reported.

2.9. Synaptosomal preparation

Regions of interest were dissected from fresh mouse brains and homogenized in ice-cold isotonic sucrose (0.32 M) buffered with HEPES (5 mM, pH 7.5). The suspension was centrifuged at $12,000 \times g$ for 20 min and the pellet resuspended in the appropriate uptake buffer (Salminen et al., 2007; Grady et al., 2001; Marks et al., 2007) and used immediately.

2.10. [³H]-Dopamine uptake and release

Release methods of Salminen et al. (2004, 2007) were used. Briefly, the crude synaptosomal pellet from striatal tissue was resuspended in dopamine uptake buffer (NaCl, 128 mM; KCl, 2.4 mM; CaCl₂, 3.2 mM; MgSO₄, 1.2 mM; KH₂PO₄, 1.2 mM; HEPES, 25 mM; pH 7.5; glucose, 10 mM; ascorbic acid, 1 mM; pargyline, 0.01 mM) at 1.6 ml/tissue from one mouse. Synaptosomes were incubated at 37 °C for 10 min before addition of [³H]DA at 1 μCi for every 0.2 ml (~100 nM), and the incubation continued for another 5 min. Subsequently, aliquots of the suspension (80 μl) were distributed onto filters and perfused at room temperature with uptake buffer containing 0.1% BSA, nomifensine (1 μM), to prevent re-uptake of dopamine, and atropine (1 μM), to prevent any possible activation of muscarinic acetylcholine receptors, at 0.7 ml/min for 10 min before stimulation with agonist for 20 s. Selected aliquots were perfused with α-CtxMII (50nM) for the last 5 min of the wash period, immediately before stimulation. This concentration of α-CtxMII is sufficient to inhibit all α6β2*-nAChR forms present in mouse striatum (Salminen et al., 2007). Fractions (~0.1 ml) were collected every 10s into 96-well plates using a Gilson F204 fraction collector (Middleton WI) for 3 min after the 10 min washout. After addition of 0.15 ml of Optiphase SuperMix scintillation cocktail, radioactivity was determined in a 1450 MicroBeta Trilux counter (Perkin Elmer Life Sciences — Wallac Oy, Turku, Finland).

2.11. [³H]-ACh uptake and release

Release methods of Grady et al. (2001) were followed with minor modifications. Briefly, the crude synaptosomal pellet from IPN tissue was resuspended in choline uptake buffer (NaCl, 128 mM; KCl, 2.4 mM; CaCl₂, 3.2 mM; MgSO₄, 1.2 mM; KH₂PO₄, 1.2 mM; HEPES, 25 mM; pH 7.5; glucose, 10 mM; 0.1% BSA) at 0.1 ml/mouse. After the addition of [³H]choline at 2 μCi for every 0.1 ml (~300 nM), the suspension was incubated at 37 °C for 30 min. Then, aliquots (20 μl) were distributed onto filters on the perfusion system at room temperature and perfused for 10 min at 0.7 ml/min with choline uptake buffer containing atropine (1 μM) before stimulation by agonist for 20 s. Collection of fractions and determination of radioactivity were as for dopamine release.

2.12. ⁸⁶Rb⁺ efflux

Nicotine-stimulated ⁸⁶Rb⁺ efflux from synaptosomes was investigated using the methods of Marks et al. (1999, 2007) with minor modifications. Briefly, Crude synaptosomes prepared from thalamus were resuspended in uptake buffer (NaCl, 140 mM; KCl, 1.5 mM; CaCl₂, 2 mM; MgSO₄, 1 mM; HEPES, 25 mM; pH 7.5; glucose, 20 mM) (350 μl/mouse thalamus). Aliquots (25 μl) of the suspension were added to 10 μl of uptake buffer containing 4 μCi ⁸⁶Rb⁺ and incubated at room temperature for 30 min. The whole sample was then collected onto filter paper (Type AE, Gelman, Ann Arbor, MI), rinsed once with 0.5 ml of uptake buffer, transferred to the perfusion apparatus, and perfused with buffer (NaCl, 135 mM; CsCl, 5 mM; KCl, 1.5 mM; CaCl₂, 2 mM; MgSO₄, 1 mM; HEPES, 25 mM; pH 7.5; glucose, 20 mM; tetrodotoxin, 50 nM; atropine 1 μM; BSA 0.1%) at 2.5 ml/min for 5 min before data collection began. Stimulation by agonist was for 5s. Effluent was pumped through a 200 μl Cherenkov cell in a β-Ram HPLC detector (IN/US Systems, Tampa, FL) to continuously monitor radioactivity.

2.13. Synaptosomal function data analysis

All synaptosomal function assays were calculated as counts exceeding basal release determined from samples immediately preceding and following stimulation (Grady et al., 2001; Salminen et al., 2004; Marks et al., 1999). Stimulated release was normalized to baseline to give units of release as a fraction of baseline. Fractions significantly over baseline for each perfusion were summed. EC_{50} values were calculated by fitting data (means of three to four experiments) to the Hill equation, or two Michaelis–Menten equations when data were biphasic. IC_{50} values were calculated from the inhibition equation (release = $R_0/(1 + [An]/IC_{50}$, where R_0 = uninhibited release and [An] is the concentration of antagonist) using the non-linear least squares algorithm in SigmaPlot 5.0 (Jandel Scientific, San Rafael, CA). The errors for the EC_{50}, IC_{50} and efficacy (as maximum activity expressed as % nicotine) are errors generated by the least-squares computational algorithm in SigmaPlot termed "sem". This "sem" reflects error of the curve fit for the entire data set rather than an sem calculated from independent determinations of these parameters.

2.14. Current recordings from GH4C1 cells

GH4C1, a stable cell line expressing the hα7-nAChR subunit, was used to measure whole-cell currents (see Dunlop et al., 2007 and Supplementary Fig. 1). After removal from the incubator, cells were washed twice with extracellular recording medium (NaCl, 130 mM; KCl, 5 mM; CaCl₂, 2 mM; MgCl₂, 2mM; glucose, 25 mM; HEPES, 10 mM, pH 7.4) and placed into a 48 channel Dynaflow chip (Cellectricon, Inc). Chips were placed on the Dynaflow stage of an inverted Zeiss microscope at room temperature. Borosilicate electrodes were filled with: Tris-phosphate dibasic, 110 mM; Tris-base, 28 mM; EGTA, 11 mM; MgCl₂, 2 mM; CaCl₂, 0.5 mM; NaATP 4 mM, pH 7.25 and had resistance of 2–5 MΩ. Currents were recorded with Axopatch 700A amplifier, filtered at 1 kHz, and sampled at 5 kHz. On average, the whole-cell recording stabilized within <5 min. Responses were evoked by moving the cell in front of the agonist-containing channel for 1 s, and 30 s washout periods were used between applications. With this method, solution exchange occurs within 10 msec.

2.15. Electrophysiological data analysis

Data were fit to a single Hill equation using Prism 5 software. Data are expressed as mean ± SEM with of 4 independent measurements. Measurements of steady state current would result in EC_{50} values shifted to the left by 10-fold or more approaching K_i values for binding (see Supplemental Fig. 1). We used peak current measurements for data presented in this paper as most likely to represent activation EC_{50} values comparable to those measured in our synaptosomal release and efflux assays.

2.16. Hypothermia and locomotor activity measurements

The methods of Tapper et al. (2007) were followed to measure the hypothermic effect of selected compounds. α4L9′A knock-in mice were used to isolate effects on α4β2*-nAChR subtypes as, in these mice, the dose required to elicit nicotine-induced hypothermia (0.01 mg/kg) is below doses that affect other subtypes as shown by a lack of effect of this dose in wild-type mice (Tapper et al., 2007). Briefly, mice were injected ip with saline, low dose nicotine (0.01 mg/kg), selected compound (agonists), or selected compound (antagonist) followed by low dose nicotine 8 min later, and body temperature was recorded in the home cage via previously implanted telemetry probes (Vital View PDT-4000 from Respironics). The maximum change in temperature within 40 min of injection was recorded.

α6L9′S transgenic mice were used to isolate effects on α6β2*-nAChR subtypes with measurements of locomotor effects. Doses of nicotine (0.1 mg/kg) that do not affect wild-type mice have marked effects in these transgenic α6 mice (Drenan et al. (2008). Briefly, baseline horizontal locomotor activity was measured in an infrared photobeam activity cage (San Diego Instruments, San Diego, CA) for 8 min before injection of either saline, low dose nicotine (0.1 mg/kg), selected compound (agonist), or selected compound (antagonist) followed by low dose nicotine 8 min later. Activity was then measured for an additional 30 min.

3. Results

This report incorporates two major themes: 1) We describe a battery of assays to assess the selectivity and activity of potential nicotinic compounds in vitro and in vivo. 2) We apply these assays to evaluate a series of potential nicotinic compounds in order to provide new data on nAChR subtype selectivity and to establish a structure-activity relationship (SAR) framework for assessing improved selectivity. The structures of the compounds tested in the current study are shown in Fig. 1.

3.1. Binding assays

Fig. 2 presents inhibition profiles using four different membrane binding assays with Compound 1 as the test compound. Panel A shows the inhibition of high affinity [¹²⁵I]-epibatidine binding to mouse
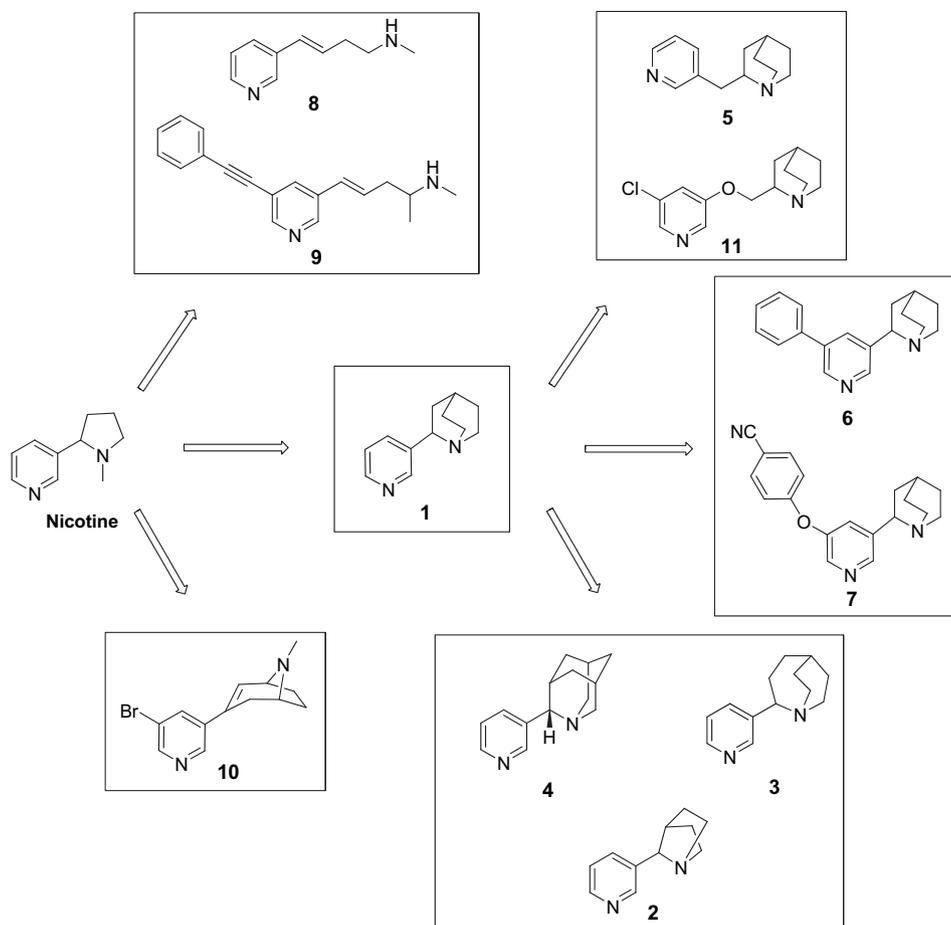
Fig. 1. Structures of compounds assayed. For Compound 1, the methylpyrrolidine ring structure of nicotine was replaced by azabicyclo[2.2.2]octane. The other compounds are related to Compound 1 in the following ways: the azabicyclo structure was modified in size to [1.2.2]heptane for Compound 2, to [3.2.2]nonane for Compound 3, and to [2.3.3.5]decane for Compound 4. An additional C was added in spacer between ring systems to generate Compound 5. An additional C as well as a 5′ halogen group were added to generate Compound 11. Additional bulky groups were added at the 5′ position of the pyridine ring for Compounds 6 and 7. The methylpyrrolidine ring of nicotine was opened up and lengthened to have 6 C between the Ns for Compound 8 and, in addition, a 5′ bulky group added for Compound 9. For Compound 10, changes include 5′ halogen groups as well as alternate ways of adding more space between the Ns.

cortical membranes, an assay that measures almost exclusively the α4β2*-nAChR. (Marks et al., 2006). The K_i for Compound 1 at this site is 0.46 nM. Panel B shows the inhibition of high-affinity [125I]-epibatidine binding to mouse IPN membranes in the presence of sufficient A-85380 to block the α4β2* sites; the site defined by the this binding is largely α3β4*-nAChR in this brain region (Whiteaker et al., 2000a) and has a K_i for Compound 1 of 4.4 nM. Panel C shows inhibition by Compound 1 of [125I]-α-Btx binding, a selective ligand for α7-nAChR, in mouse hippocampal membranes (Marks et al., 1998). The K_i for Compound 1 at this site is 7.6 nM. Panel D represents inhibition by Compound 1 of [125I]-α-CtxMII binding, a selective ligand for α3β2* and α6β2* to mouse membranes from combined regions, striatum (ST), olfactory tubercles (OT), and superior colliculus (SC), which are all relatively high in the α6β2*-nAChR subtype and low in α3β2* (Salminen et al., 2005). The K_i for Compound 1 at this site is 1.14 nM.

3.2. Functional assays

The affinity measurements above provide some information on the interaction of ligands with these receptor subtypes, but give no indication of their functional activity. Fig. 3 presents functional data from appropriate biochemical (Fig. 3A, B, C) or electrophysiological (Fig. 3D) assays for each of the four nAChR subtypes, again using Compound 1 for illustration. For the data in panels A, B and C,

functional responses were measured using mouse brain synaptosomes. The activity of a concentration of nicotine, maximal for each assay and assessed in the same assays, is also shown and has been used to estimate relative efficacy. EC_{50} values were determined by fits to the Hill equation or, for biphasic curves, to two Michaelis−Menton equations.

Panel A of Fig. 3 shows $^{86}Rb^+$ efflux stimulated from mouse thalamic synaptosomes by the indicated concentrations of Compound 1. A biphasic concentration-response curve was observed. Previous data show that the higher agonist-sensitivity (HS) component also has higher sensitivity to block by DHβE (2 μM) (Marks et al., 1999). We therefore isolated the DHβE-sensitive portion by subtracting the responses in the presence of DHβE from the total responses; the inset shows the calculated HS α4β2* responses. The EC_{50} value for this HS form is assessed from either this plot of the DHβE-sensitive component or by the higher-affinity portion of the biphasic plot. The lower sensitivity (LS) form is assessed from the curve with DHβE present and by the component of the concentration-response curve elicited by higher agonist concentrations. Compound 1 is a partial agonist at both the HS and LS forms with efficacies of 31% and 29% relative to the test concentrations of nicotine, respectively. Corresponding EC_{50} values are 0.043 μM and 5.5 μM, much lower than those reported for nicotine [1.4 μM and 130 μM (Marks et al., 1999)].
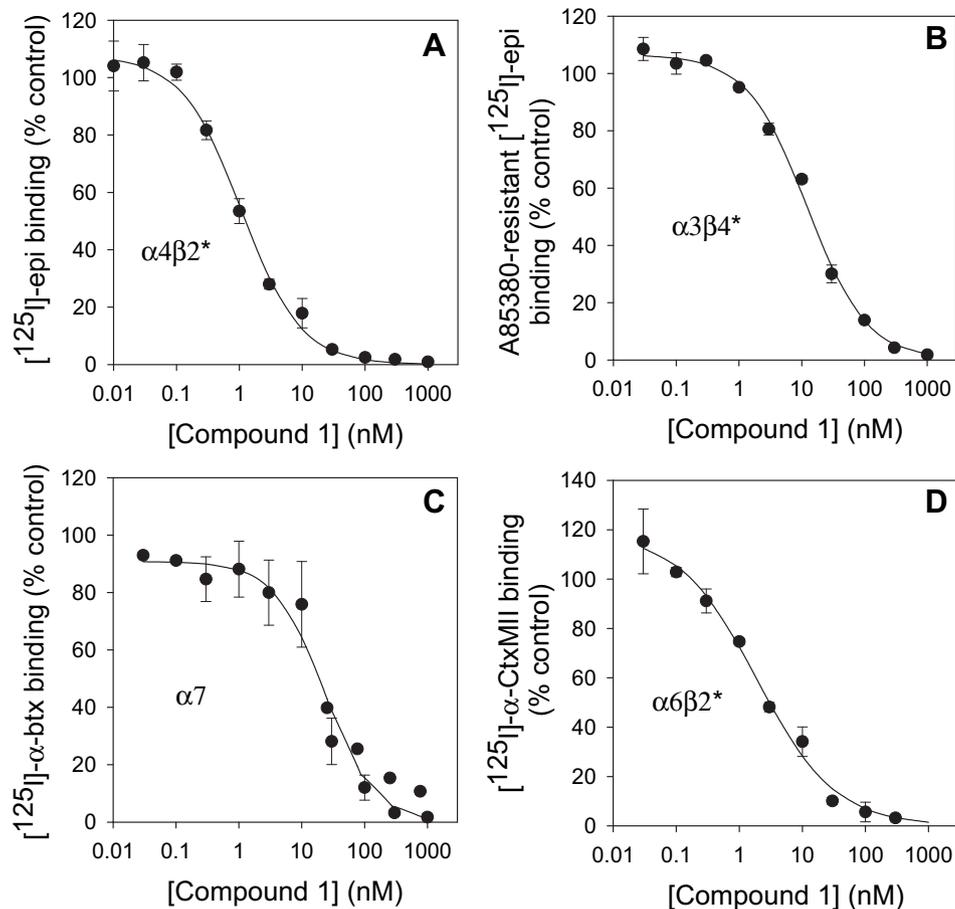
Fig. 2. Inhibition of membrane binding to assess K_i values at various subtypes of nAChR. Panel A: Inhibition of binding to $\alpha 4\beta 2^*$-nAChR by Compound 1. High affinity [^{125}I]-epibatidine binding (at 200 pM) in cortical membranes, was inhibited by 11 concentrations of Compound 1 from 0.01 nM to 1000 nM; data points are means ± sem for 6 experiments. $IC_{50} = 1.17 \pm 0.14$ nM ($Ki = 0.46 \pm 0.06$ nM). Panel B: Inhibition of binding to $\alpha 3\beta 4^*$-nAChR by Compound 1. The data were gathered with membranes prepared from IPN, a region high in $\alpha 3\beta 4^*$-nAChR, using [^{125}I]-epibatidine with A-85380 added to block binding to $\beta 2^*$-nAChR. Data points are means ± sem for 3 experiments. $IC_{50} = 12.44 \pm 2.20$ nM ($K_i = 4.4 \pm 3.6$ nM). Panel C: Inhibition of binding to $\alpha 7$-nAChR by Compound 1. [^{125}I]-α-bungarotoxin binding to membranes from HP was inhibited by various concentrations of Compound 1. Data points are means ± sem for 4 experiments. $IC_{50} = 30.81 \pm 8.39$ nM ($Ki = 7.6 \pm 1.9$ nM). Panel D: Inhibition of binding to $\alpha 6\beta 2^*$-nAChR by Compound 1. [^{125}I]-α-CtxMII binding to membranes of combined ST, OT and SC, areas high in $\alpha 6^*$-nAChR, was inhibited by 9 concentrations of Compound 1. Data points are means ± sem for 3 experiments. $IC_{50} = 1.9 \pm 0.6$ nM ($K_i = 1.14 \pm 0.35$ nM).

Panel B of Fig. 3 shows results of the Compound 1 stimulated release of [^{3}H]-DA from mouse striatal synaptosomes. The three plots represent total release mediated by a combination of various $\beta 2^*$-subtypes, the portion resistant to inhibition by 50 nM α-CtxMII (virtually all HS form of $\alpha 4\beta 2^*$ as the highest concentration assessed was 0.3 μM), and the difference which represents the portion sensitive to α-CtxMII ($\alpha 6\beta 2^*$) (Champtiaux et al., 2002, 2003; Salminen et al., 2004). Compound 1 is a partial agonist for the α-CtxMII-resistant ($\alpha 4\beta 2^*$) component with an efficacy 28% that of nicotine and an EC_{50} value of 0.034 μM. In contrast, Compound 1 is a full agonist at the α-CtxMII-sensitive ($\alpha 6\beta 2^*$) component with an efficacy 109% that of nicotine and an EC_{50} value of 0.0074 μM. The EC_{50} values for both components are considerably lower than the corresponding values for nicotine [1.6 μM and 0.77 μM, respectively (Salminen et al., 2004)].

Panel C of Fig. 4 shows the Compound 1-stimulated release of [^{3}H]-ACh from mouse IPN synaptosomes, an assay that measures function of the $\alpha 3\beta 4^*$-nAChR subtype (Grady et al., 2001). Compound 1 is a full agonist in this assay with a maximal response 106% that of nicotine and an EC_{50} value of 0.43 μM, which is significantly lower than the EC_{50} value for nicotine (64 μM, Grady et al., 2001) but substantially higher than that for HS $\alpha 4\beta 2^*$- or $\alpha 6\beta 2^*$-nAChR mediated responses.

Responses mediated by $\alpha 7$-nAChRs are more reliably measured by electrophysiology in transfected cell lines than by biochemical assays in mouse brain synaptosomes. Panel D of Fig. 4 shows data for peak whole-cell current evoked from patch-clamped GH4C1 cells expressing rat $\alpha 7$-nAChR. These data are expressed as % maximal ACh response. In comparison to ACh, nicotine was a full agonist for this activity (data not shown; 100% max at 200 μM). Compound 1 is also a nearly full agonist in this assay with a maximal response 89% that of nicotine. The EC_{50} value of 0.66 μM was the highest of the four responses measured.

3.3. Screening of compounds

Each of the compounds represented in Fig. 1 was assayed for each of the measures illustrated in Figs. 2 and 3, respectively. K_i values for inhibition of binding of these compounds are compiled in Table 1. Fig. 4A presents these affinity values on log molar scales, in a plot that emphasizes each compound's rank order for each of the four subtypes. Most of the compounds evaluated had higher affinity for the $\alpha 4\beta 2^*$-nAChRs relative to the other subtypes, as is typical for most reported nicotinic ligands. For function (assays in Fig. 3), all compounds were initially screened for agonist activity. Several compounds had no agonist activity; and were tested for antagonist activity as measured by the inhibition of nicotine-stimulated responses, and K_i values determined. The data on functional activity are compiled in Tables 2 and 3 and also represented graphically, as
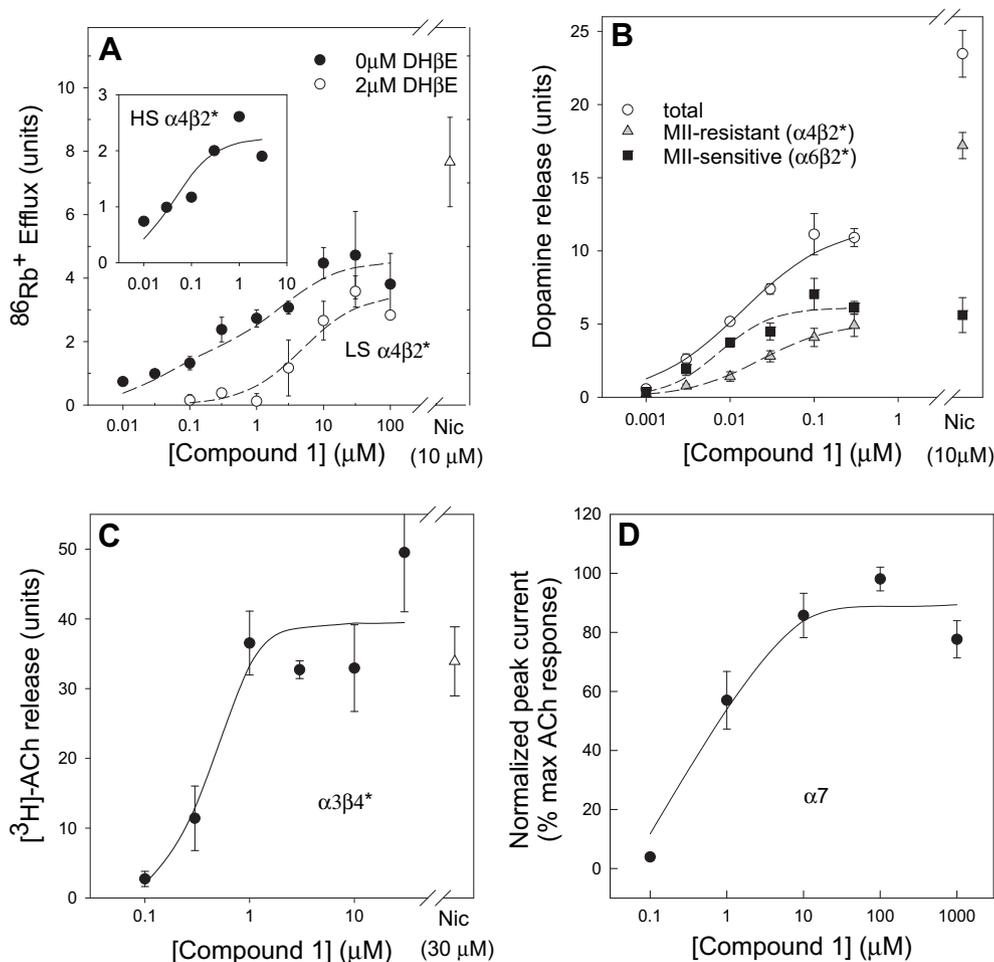
Fig. 3. Functional assays for agonist activity of Compound 1 at various subtypes of nAChR. Panel A: Function of $\alpha4\beta2^*$-nAChR measured by high sensitivity $^{86}Rb^+$ efflux from thalamic synaptosomes. EC_{50} values were determined by either high affinity portion of a 2-site fit of data without $DH\beta E$ (37 ± 25 nM), or by subtraction of the $DH\beta E$-resistant activity (inset) fit to a single site (43 ± 25 nM). Panel B: Measurement of function at $\alpha4\beta2^*$-nAChR by α-CtxMII-resistant $[^3H]$-dopamine release and $\alpha6\beta2^*$-nAChR by α-CtxMII-sensitive $[^3H]$-dopamine release from striatal synaptosomes. EC_{50} values by curve fit, 34 ± 7 nM and 7.4 ± 1.3 nM, respectively. Panel C: Measurement of function at $\alpha3\beta4^*$-nAChR by $[^3H]ACh$ release from IPN synaptosomes. EC_{50} values by curve fit, 430 ± 190 nM. Panel D: Measurement of function at $\alpha7^*$-nAChR by relative peak current in GH4C1 cells. EC_{50} values by curve fit, 660 ± 370 nM. All data shown are means $\pm$ sem from 4 experiments.

potency values (EC_{50} or K_i) in Fig. 4B and efficacy relative to nicotine (as a percentage) in Fig. 4C. For this representation, a fully efficacious compound has 100% maximum activity as compared to the activity of nicotine, while an antagonist that fully blocks the effect of nicotine is plotted at −100%. Several compounds have partial activity (between 0 and 100) while a few are more efficacious than nicotine (over 100). A value of 0 indicates that no agonist or antagonist activity was detected. In addition to compounds 1–11, values for a number of common nicotinic compounds as well as varenicline are presented for comparison in Fig. 4A, B and C (see also Tables 1–3 for nicotine and varenicline).

3.4. $\alpha4\beta2^*$-nAChR-mediated responses

From the assays shown in panels A and B of Fig. 3, we can measure potency and efficacy relative to nicotine for activity mediated by the $\alpha4\beta2^*$-subtype by two independent methods: HS $^{86}Rb^+$ efflux and α-CtxMII-resistant $[^3H]$-DA release. These two measures of $\alpha4\beta2^*$ potency showed good agreement: a scatterplot on logarithmic axes has a regression slope of 0.98 ± 0.08 and a correlation coefficient of 0.96 (Fig. 5A). The mean ratio of the points (0.97 ± 0.14) does not differ from 1. The accuracy of these methods with a limited number of replicates appears adequate to ascertain functional potency

within a ∼3−10-fold difference. For the purpose of identifying a compound useful for differentially activating or inhibiting subtypes of nAChRs, this level of accuracy should suffice.

Functional responses mediated by $\alpha4\beta2^*$-nAChR measured within the series of compounds shown in Fig. 1 reveal that only four of the eleven compounds (including Compound 1) are agonists (see Fig. 4C). Compound 8 was unique in that it had higher efficacy than nicotine at $\alpha4\beta2^*$-elicited $[^3H]$-DA release (150%) and at $\alpha4\beta2^*$-nAChR mediated $^{86}Rb^+$ efflux (254%), but with relatively high EC_{50} values (14.8 and 14.6 μM, respectively, see Fig. 4B and Tables 2 and 3). Compound 2 is a partial agonist (64% and 21%), albeit much less potent than Compound 1 (EC_{50} 1.04 μM and 0.32 μM). Finally, Compound 10 was a partial agonist (37% efficacy for α-CtxMII-resistant $[^3H]$-DA release and 63% for $^{86}Rb^+$ efflux), but intermediate potency (0.18 μM and 0.06 μM) compared to Compound 1 and Compound 2.

3.5. $\alpha6\beta2^*$-nAChR-mediated responses

Functional responses mediated by $\alpha6\beta2^*$-nAChR, as the α-CtxMII-sensitive component of $[^3H]$-DA release, measured within the series of compounds shown in Fig. 1 reveal that only three of the eleven compounds (including Compound 1) are agonists. Compound 10 is
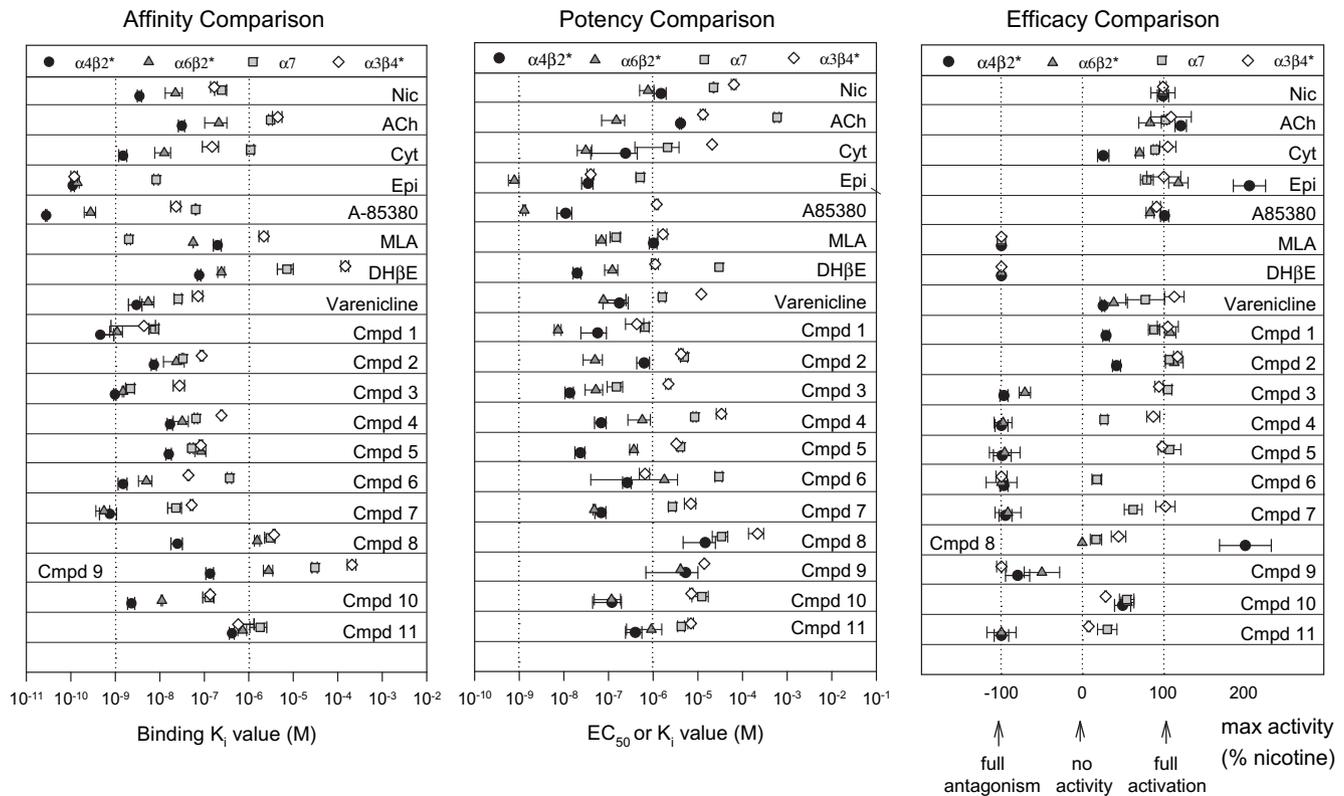
Fig. 4. Comparison of parameters determined by *in vitro* assays. Panel A compares affinity for four subtype classes of nAChRs for a number of commonly studied nicotinic compounds, varenicline, and the 11 compounds shown in Fig. 1. K_i values for inhibition of various selective binding assays are plotted. Dotted lines indicate 1 nM and 1 μM. Data for commonly studied nicotinic compounds are from Whiteaker et al. (2000a), Marks et al. (1986, 1993, 2006), Salminen et al. (2005), unpublished data NBF, MJM. Panel B compares potency of compounds for activation (EC$_{50}$ values) or inhibition (K_i values) of four subtype classes of nAChR. Dotted lines indicate 1 nM and 1 μM. Data for commonly studied nicotinic compounds are from Salminen et al. (2004), Grady et al. (2001), Marks et al. (1999), unpublished data NBF, MJM. Panel C compares efficacy for compounds as compared to nicotine for activation or inhibition of four subtype classes of nAChR. Dotted lines indicate efficacy values of 100% (equal to nicotine), 0 efficacy (no functional activity), and −100% (full antagonism). Data for commonly studied nicotinic compounds are from Salminen et al. (2004), Grady et al. (2001), Marks et al. (1999), unpublished data NBF, MJM.

Table 1
Affinity of compounds for various binding sites as K_i values (nM).

Compound	α4β2*	α6β2*	α7	α3β4*
Nicotine	3.50 ± 0.37[a]	22.6 ± 9.3[b]	244 ± 73	167 ± 28
		44.9 ± 8.8		
Varenicline	2.99 ± 1.01	5.5 ± 1.9	42 ± 5	72.9 ± 18.9
		5.6 ± 1.9		
Compound 1 TC2429/RJR2429	0.46 ± 0.06	1.14 ± 0.35	7.6 ± 1.9	4.4 ± 3.6
		1.3 ± 0.2		
Compound 2	7.42 ± 0.98	23.7 ± 11.6	32.9 ± 1.3	88 ± 8
		25.2 ± 3.1		
Compound 3 TC1698	0.98 ± 0.06	1.48 ± 0.07	2.2 ± 0.5	28 ± 8
Compound 4	16.9 ± 2.4	32.3 ± 12.0	64.5 ± 5.5	244 ± 12
Compound 5	16.1 ± 2.3	85.2 ± 23.6	51.9 ± 5.0	84 ± 8
		83.3 ± 11.1		
Compound 6 TC6951	1.54 ± 0.34	4.8 ± 1.67	367 ± 44	44 ± 2
Compound 7 TC2242	0.75 ± 0.31	0.56 ± 0.19	23.4 ± 7.9	52 ± 4
Compound 8 RJR2403/TC2403	25.0 ± 7.2	1550 ± 210	3070 ± 800	3720 ± 200
		228 ± 41		
Compound 9	134 ± 26	2790 ± 660	30699 ± 4100	210000 ± 46000
		2329 ± 443		
Compound 10	2.31 ± 0.42	11.1 ± 0.4	128 ± 36	136 ± 4
		2.2 ± 0.3		
Compound 11	418 ± 53	732 ± 161	1810 ± 740	580 ± 60

Data are K_i values (nM) for inhibition of: α4β2* measured by [^{125}I]epi binding to mouse cortical membranes; α6β2* first number measured by [^{125}I]-α-CtxMII binding to combined mouse ST/OT/SC membranes and, for those compounds with a second number, by [^{125}I]epi binding to combined mouse ST/OT/SC membranes from α4 null mutant mice; α7 measured by [^{125}I]-α-Btx binding to mouse hippocampal membranes. (See methods section).

[a] From Whiteaker et al. (2000a).
[b] From Salminen et al. (2005).

Table 2
Potency of compounds for subtypes of nAChR as EC_{50} or K_i values (nM).

Compound	α4β2*	α6β2*	α7	α3β4*
Nicotine	1610 ± 190[a] 1390 ± 420[c]	770 ± 270[a]	22600 ± 540	64400 ± 7900[b]
Varenicline	50 ± 12 300 ± 100	77 ± 169	1600 ± 250	12000 ± 300
Compound 1 RJR2429/TC2429	34 ± 7 43 ± 25	7.4 ± 1.3	660 ± 150	430 ± 190
Compound 2	1040 ± 280 320 ± 100	50 ± 23	4970 ± 871	4200 ± 500
Compound 3 TC1698	14 ± 3 # 13 ± 1 #	52 ± 22 #	150 ± 57	2200 ± 300
Compound 4	78 ± 23 # 59 ± 12 #	570 ± 299 #	8500 ± 720	34000 ± 8000
Compound 5	16 ± 4 # 31 ± 4 #	370 ± 73 #	4100 ± 472	3300 ± 100
Compound 6 TC6951	230 ± 29 # 298 ± 64 #	1780 ± 1741 #	29000 ± 5400	660 ± 170 #
Compound 7 TC2242	66 ± 2 # 71 ± 20 #	48 ± 3 #	2700 ± 490	7000 ± 2000 #
Compound 8 RJR2403/TC2403	14800 ± 10100 14600 ± 4900	na	34000 ± 12900	218000 ± 81000
Compound 9	3900 ± 3400 # 6800 ± 2400 #	4100 ± 83 #	naa	14000 ± 300 #
Compound 10	178 ± 94 59 ± 37	117 ± 69	12270 ± 4900	7200 ± 600
Compound 11	490 ± 198 # 315 ± 108 #	910 ± 656 #	4260 ± 730	7000 ± 1000

Data are EC_{50} values (nM) for activation or K_i values (nM and marked with #) for inhibition of nicotine-stimulated activation and are from curve-fits. For α4β2*, two numbers are given, the 1st is for the [³H]DA release assay, the 2nd for the ⁸⁶Rb⁺ efflux assay. na = no activity, naa = no agonist activity.
[a] From Salminen et al. (2004).
[b] From Grady et al. (2001).
[c] From Marks et al. (1999).

Table 3
Efficacy of compounds for activation as % nicotine effect for activation or for % inhibition of nicotine at subtypes of nAChR.

Compound	α4β2*	α6β2*	α7	α3β4*
Varenicline	26 ± 2% 29 ± 3%	39 ± 17%	78 ± 24%	114 ± 12%
Compound 1 RJR2429/TC2429	28 ± 2% 31 ± 4%	109 ± 7%	89 ± 7%	106 ± 13%
Compound 2	64 ± 5% 21 ± 2%	114 ± 11%	108 ± 5%	118 ± 5%
Compound 3 TC1698	−94 ± 5% −100 ± 3%	−71 ± 7%	106 ± 5%	95 ± 5%
Compound 4	−100 ± 8% −100 ± 4%	−98 ± 11%	27 ± 4%	88 ± 8%
Compound 5	−98 ± 11% −100 ± 3%	−96 ± 19%	108 ± 14%	99 ± 2%
Compound 6 TC6951	−94 ± 2% −100 ± 5%	−100 ± 19%	18 ± 6%	−100 ± 7%
Compound 7 TC2242	−90 ± 8% −100 ± 5%	−92 ± 16%	63 ± 11%	103 ± 12%
Compound 8 RJR2403/TC2403	150 ± 32% 254 ± 21%	0%	17 ± 7%	45 ± 9%
Compound 9	−80 ± 15% −100 ± 5%	−50 ± 22%	naa	−100 ± 6%
Compound 10	37 ± 4% 63 ± 10%	56 ± 8%	55 ± 9%	29 ± 1%
Compound 11	−100 ± 9% −100 ± 6%	−100 ± 18%	31 ± 12%	8 ± 2%

In this representation, negative numbers signify antagonists and % values are for maximum inhibitory effect on nicotine-stimulated activity. Positive numbers are agonists and values represent maximum effect as compared to nicotine. Nicotine response at 10 μM was defined as 100% for α4β2* and α6β2*-nAChRs, 30 μM was 100% for α3β4*, and for α7, 100% was at 200 μM nicotine and all were measured in the same experiments as the compound. All values are as maximal release or inhibition from curve-fits of the data. naa = no agonist activity.

a potent (EC_{50} = 0.12 μM) partial agonist with 56% of the efficacy of nicotine. Compound 2 is a potent full agonist with an EC_{50} value of 0.050 μM. In contrast to the α4β2*-mediated responses where Compound 8 is more efficacious than nicotine, Compound 8 displays no measurable activity on α-CtxMII-sensitive DA release. Interestingly, α6β2*-nAChR appear to be activated by lower concentrations of many agonists than α4β2*-nAChR (see Fig. 4B and Table 2) even though these same agonists have higher affinity for α4β2* sites in binding assays (see Fig. 4A and Table 1). Comparing data in Fig. 4A and B, this pattern, where a compound has higher affinity for α4β2*-nAChR than α6β2*-nAChR for binding, but lower or equal potency for activation, is seen for the agonists, nicotine, ACh, cytisine, epibatidine, A85380, varenicline and compounds 1, 2 and 10. In contrast, antagonists that have highest affinity for α4β2*-nAChR also have highest potency for inhibition at that subtype. In addition, compound 8 has no functional activity at α6β2*-nAChR, so it cannot be compared. It seemed possible that for α6β2*-nAChR, measurements of inhibition of binding of an antagonist ([¹²⁵I]-αCtxMII) might differ from inhibition of binding of an agonist ([¹²⁵I]-epibatidine), possibly explaining the relatively lower affinities measured for α6β2* sites using α-CtxMII, an antagonist. Therefore, we compared data collected by two independent methods for binding to α6β2*-nAChR sites to check accuracy of the results of this screening method. The first method, illustrated in Fig. 2D, is inhibition of [¹²⁵I]-αCtxMII binding; the alternate method, using a similar membrane preparation from mice with the α4 subunit null mutation, assessed inhibition of high affinity [¹²⁵I]-epibatidine binding to the remaining, presumably α6β2*, nAChRs. In ST, ~10% of high affinity [¹²⁵I]-epibatidine binding remains in the α4 subunit null mouse; and in OT, ~8% remains (Marks et al., 2007). In addition, the α4 subunit null mouse has ~50% lower [¹²⁵I]-α-CtxMII binding in these regions, although the affinity for α-CtxMII is unchanged (Salminen et al., 2005, 2007). In a comparison of K_i values determined by the two methods
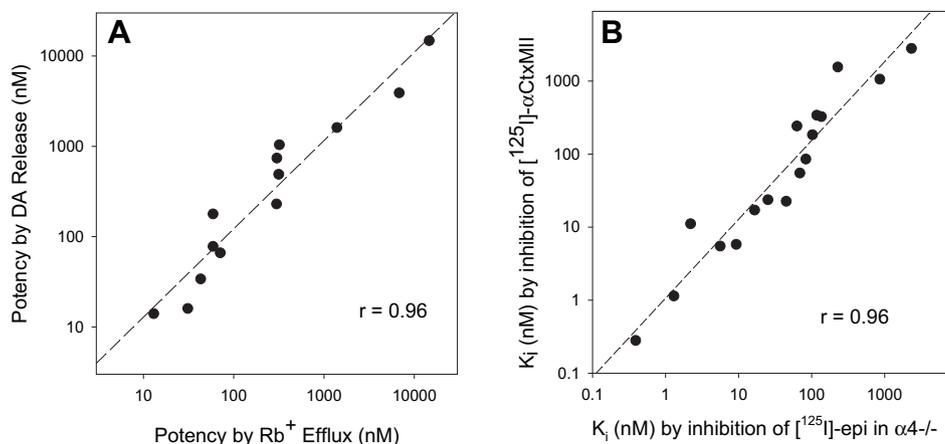
Fig. 5. Correlations of independent methods for assessing affinity and potency. Panel A: Comparison of potency (EC_{50} values) for stimulating $\alpha4\beta2*$nAChR by measurement of $^{86}Rb^+$ efflux from thalamic synaptosomes vs. stimulating [^{3}H]-dopamine release resistant to α-CtxMII from striatal synaptosomes. The calculated slope is 0.98 ± 0.08, $r = 0.96$, and the mean ratio of the points (0.97 ± 0.14, mean $\pm$ sem, x/y) does not differ from 1. Panel B: Comparison of inhibition constants (K_i values, M) for nicotinic compounds measured by inhibition of [^{125}I]-αCtxMII binding to membranes prepared from mouse striatum, olfactory tubercle and superior colliculus vs. constants measured by inhibition of [^{125}I]-epibatidine binding to membranes prepared from striata and olfactory tubercles of $\alpha4$ subunit null mutant mice. The calculated slope is 1.08 ± 0.08, $r = 0.96$, and the mean ratio of the points (0.88 ± 0.13, mean $\pm$ sem, x/y) does not differ from 1.

(see Table 1 for values $\pm$ sem for both methods for those compounds assayed both ways), the regression slope on logarithmic axes was 1.08 ± 0.08 with a correlation coefficient of 0.96 (Fig. 5B). Furthermore, the mean ratio of the K_i values determined by the two methods (0.88 ± 0.13) is not significantly different from 1. Therefore, we conclude that the lower affinity values measured for $\alpha6\beta2*$-nAChR sites are not an artifact of measuring binding affinities with [^{125}I]-α-CtxMII rather than with [^{125}I]-epibatidine, since measurements of $\alpha6\beta2*$ binding affinity for a number of compounds using $\alpha4$ subunit null mutant membranes with [^{125}I]-epibatidine resulted in the same K_i values as those measured with [^{125}I]-α-CtxMII (Fig. 5B).

3.6. α7-nAChR-mediated responses

All of the compounds tested, except Compound 9 which was inactive, showed at least some agonist activity for $\alpha7$-nAChR-mediated function (Fig. 4C and Table 3). Compound 2 is a full agonist. However, like Compound 1, the EC_{50} value for this compound (4.97 μM) was significantly higher than the corresponding value observed for $\alpha4\beta2*$ (0.68 μM) and $\alpha6\beta2*$ (0.05 μM) responses. Compounds 3 and 5 are full agonists with EC_{50} values of 0.15 and 4.1 μM, respectively. Partial agonist activity was noted for the remaining compounds with efficacies ranging from 17% to 63%. In general, EC_{50} values for $\alpha7$-nAChR activation were markedly higher than those for $\alpha4\beta2*$- and $\alpha6\beta2*$-nAChR mediated responses, although the ratio of EC_{50} to K_i value (77 ± 14, $n = 11$) was similar to that for $\alpha4\beta2*$-nAChR.

3.7. α3β4*-nAChR-mediated responses

$\alpha3\beta4*$-nAChR mediated responses were measured by [^{3}H]-ACh release from IPN synaptosomes. Nine of the 11 compounds tested show some agonist activity (Fig. 4C and Table 3). Compounds 1, 2, 3, 4, 5 and 7 were full or nearly full agonists, while Compounds 8, 10 and 11 were partial agonists. The EC_{50} for Compound 8 was a very high 218 μM. Both Compound 6 and Compound 9 were full antagonists, with Compound 6 exhibiting high potency ($K_I = 0.66$ μM).

3.8. Evaluation of effect of structural differences on interaction with nAChR subtypes

Compound 8 and Compound 9 are both classified as meta-nicotines, analogs of nicotine in which the pyrrolidine ring is opened

and a double bond introduced adjacent to the pyridine. This results in a more flexible molecule than nicotine and increases the distance from the cationic center to the hydrogen bond acceptor. Relative to nicotine, Compound 8 possesses decreased affinity at $\alpha4\beta2*$, $\alpha7$ and $\alpha6\beta2*$ subtypes. Like nicotine, Compound 8 displayed selectivity for the $\alpha4\beta2*$ subtype, consistent with previous reports (Bencherif et al., 1996). In terms of functional activity, Compound 8 is even more efficacious than nicotine at $\alpha4\beta2*$, but displays no measurable activity at $\alpha6\beta2*$ and weak partial activity at $\alpha3\beta4*$ and $\alpha7$-subtypes.

Introduction of a phenyl ring at the 5' position of the pyridine (Compound 9) through an alkyne linker further reduced binding affinity across subtypes, but maintained selectivity for the $\alpha4\beta2*$ sites. This modification also resulted in antagonism at all subtypes, though antagonism at $\alpha6\beta2*$ was partial ($\sim 50\%$ inhibition). It remains to be seen whether this compound selectively inhibits one of the complex $\alpha6\beta2*$-nAChR subtypes (i.e., $\alpha6*$ receptors with or without an $\alpha4$ subunit incorporated).

Constraining the basic structural elements of Compound 8 (pyridine, alkene, aminomethyl) into an azabicyclo[3.2.1]octene ring and adding a 5'-bromo substituent results in Compound 10. This conformational constraint increased the binding affinity by more than an order of magnitude at all four subtypes, while still retaining modest selectivity for $\alpha4\beta2*$. These modifications also returned partial agonist activity at all subtypes measured. In fact, Compound 10 appears unique among the compounds studied here in having partial agonist activity across all subtypes. Relative to Compound 8, Compound 10 exhibited significantly reduced efficacy (25% of Compound 8) at both α-CtxMII-resistant DA release and $\alpha4\beta2*$-mediated $^{86}Rb^+$ efflux, but increased the potency 83- and 250-fold, respectively. Compound 10 demonstrated considerable potency-based functional selectivity (~ 100-fold) for the $\beta2*$ (both $\alpha4$ and $\alpha6$) containing subtypes over both $\alpha7$ and $\alpha3\beta4*$-subtypes. This selectivity might be expected to reduce side effect liabilities relative to less selective ligands, particularly with regard to the $\alpha3\beta4*$ subtype.

Replacement of the pyrrolidine ring of nicotine by the azabicyclo[2.2.2]octane (quinuclidine) ring system (Compound 1) has multiple steric and electronic effects. The basicity of the cationic center nitrogen is greatly enhanced, steric bulk around the cationic center is also greatly increased, and the resulting molecule is considerably more rigid. These structural modifications conferred enhanced binding affinity across all four receptor subtypes ($\sim 10-40$-fold increase). With respect to efficacy and potency, Compound 1 is

a partial agonist at both DA release (28%) and Rb efflux (31%) measures of $\alpha4\beta2^*$ function, but is very potent (EC$_{50}$ 0.034 μM for [^{3}H]–DA release, 0.043 μM for ^{86}Rb$^+$ efflux). Although the efficacy for $\alpha4\beta2^*$ function by Compound 1 is fairly low, this compound is a potent, full agonist for the component of dopamine release mediated by $\alpha6\beta2^*$ (109%, 0.0074 μM EC$_{50}$). Compound 1 is highly efficacious at the $\alpha3\beta4^*$ and $\alpha7$ subtypes (106% and 89%, respectively), but the EC$_{50}$ values (0.43 μM and 0.66 μM) are 10- to 100-fold higher than those for $\alpha4\beta2^*$ and $\alpha6\beta2^*$-receptors. By this measure, Compound 1 represents a functionally highly selective and efficacious $\alpha6\beta2^*$ agonist, though less selective by binding affinity measures.

The Compound 1 template was further elaborated at the 5′-pyridine position, to explore the effects of aromatic bulk across the various receptor subtypes. Introduction of a phenyl ring gave Compound 6, which exhibited decreased affinity for all four subtypes (Fig. 4A and Table 1). This decrease was modest ($\sim$4–5–fold) for $\alpha4\beta2^*$ and for $\alpha6\beta2^*$, but approximately 10-fold for $\alpha3\beta4^*$. The largest effect was noted for the $\alpha7$ subtype, where affinity decreased approximately 50-fold. The presence of the phenyl ring markedly affects functional activity for several subtypes. Agonism was abolished at $\alpha4\beta2^*$ or $\alpha6\beta2^*$, resulting in full, potent antagonists. Compound 6 was also a full antagonist at $\alpha3\beta4^*$, but retained weak partial agonist activity at $\alpha7$ (18% E$_{max}$, 29 μM).

Extension of the 5′-position of Compound 1 with a 4-cyano-phenoxy group provided Compound 7. This modification was quite well tolerated, retaining affinity comparable to that of the parent Compound 1 for $\alpha4\beta2^*$, $\alpha6\beta2^*$ and $\alpha7$ subtypes, while decreasing affinity for the $\alpha3\beta4^*$ subtype by $\sim$10-fold. Like Compound 6, Compound 7 was a potent, full antagonist at $\alpha4\beta2^*$ and $\alpha6\beta2^*$. In fact, at $\alpha6\beta2^*$ it was 40 times more potent than Compound 6. At $\alpha3\beta4^*$ and $\alpha7$, the agonism profile more closely matched that of parent Compound 1, with full agonism at $\alpha3\beta4^*$ and partial at $\alpha7$ (103% and 63%, respectively).

Compound 5 and Compound 11 both retain the azabicyclo[2.2.2] octane ring of Compound 1, but extend the pyridine group away from the basic nitrogen by a carbon or one carbon and one oxygen atom, respectively. For Compound 5, the affinity was markedly decreased at all four sites relative to Compound 1. The smallest change was observed for $\alpha7$ ($\sim$7-fold reduction), while the $\alpha6\beta2^*$ affinity decreased 80-fold. Compound 5 was a full antagonist at both $\alpha4\beta2^*$ and $\alpha6\beta2^*$-subtypes while maintaining full but less potent agonism at the $\alpha7$ and $\alpha3\beta4^*$-subtypes.

Additional extension of the methylene spacer by introduction of an oxygen atom and translocating the spacer from the 2- to the 3-position on the quinuclidine yielded Compound 11 (which also has a 5′-Cl substitution in the pyridine ring). This further reduced affinity at all four binding sites compared to Compound 5 (further 7- to 26-fold decrease). Similar to Compound 5, full antagonism was observed at $\alpha4\beta2^*$ and $\alpha6\beta2^*$, but potency was reduced somewhat (16 and 2-fold, respectively). Surprisingly, a loss of agonism was observed at both $\alpha7$ and, more profoundly, $\alpha3\beta4^*$ (E$_{max}$ = 31% and 8%, respectively). We cannot yet distinguish the individual contributions of the 5-chloro substituent and the oxygen atom relative to the increase in linker length alone, because the corresponding analogs were not available for evaluation.

A one-carbon reduction in the bridging ethyl group of Compound 1 afforded the corresponding 1-azabicyclo[2.1.1]heptane (Compound 2). This resulted in markedly reduced binding affinity for all four sites: $\sim$20-fold at $\alpha4\beta2^*$, $\alpha6\beta2^*$ and $\alpha3\beta4^*$. Compound 2 did retain agonism at the $\alpha6\beta2^*$, $\alpha7$ and $\alpha3\beta4^*$ subtypes as well as partial agonism at $\alpha4\beta2^*$, but was less potent than Compound 1. Compound 2 also retained the full, potent agonism at $\alpha6\beta2^*$ observed for Compound 1 (114%, 0.050 μM), and the $\alpha6\beta2^*$ functional selectivity is even higher due to the reduced potency at $\alpha4\beta2^*$-subtype.

A corresponding one-carbon increase in the bridging ethyl group of Compound 1 afforded the corresponding 1-azabicyclo [3.2.2]nonane (Compound 3). The affinity of Compound 3 resembled Compound 1; however, a notable 6-fold reduction in affinity at the $\alpha3\beta4^*$ site was achieved. The functional profile again resembled that observed for the previously discussed analogs: a shift to antagonism at $\alpha4\beta2^*$ and $\alpha6\beta2^*$, but retention of $\alpha7$ and $\alpha3\beta4^*$ full agonism. In $\alpha6\beta2^*$ [^{3}H]-DA release, assays, only partial antagonism was observed for Compound 3 (-71% I$_{max}$, 0.052 μM). One possible explanation for this observation is selective inhibition of only one of the complex $\alpha6\beta2^*$-nAChR subtypes.

Finally, addition of two carbons to the Compound 1 ring system and altering the bridge connectivity produced the highly constrained 1-azatricyclo[3.3.1.13,7]decane (aza-adamantane), Compound 4. The binding affinity of Compound 4 was markedly reduced across all subtypes, quite similar to the profile observed for Compound 2. The increase in steric bulk surrounding the cationic center apparently resulted in full antagonism of $\alpha4\beta2^*$. At the $\alpha6\beta2^*$ subtypes, full antagonism was also observed, in contrast to the partial antagonism of Compound 3. Compound 4 exhibited a reduction of efficacy and large loss of potency at $\alpha3\beta4^*$ and $\alpha7$ (88%, 34 μM and 27%, 8.5 μM, respectively). This efficacy-potency shift again affords a selective antagonist. The potency is highest for $\alpha4\beta2^*$ (0.069 μM), with some antagonism for $\alpha6\beta2^*$ (0.57 μM), and less at $\alpha7$ (34 μM) and $\alpha3\beta4^*$ (8.5 μM).

3.9. Evaluation of effects of compounds in vivo

In order to assess the effects of selected compounds in vivo, we used mice with gain-of-function mutations in $\alpha4$ and $\alpha6$ subunits. Mice with the $\alpha4$L9′A or $\alpha6$L9′S mutations respond to very low concentrations of nicotine that have no measurable effect in wild type mice and allow an assessment of whether a compound is bioavailable as well as whether it activates or inhibits a specific subtype of nAChR in vivo. For the $\alpha4$L9′A mice, injection of 0.03 mg/kg nicotine produces a 3 °C temperature decrease, while this dose elicits no hypothermia in wild type mice (Tapper et al., 2007). Thus this procedure measures an effect of nicotine restricted to the $\alpha4^*$-nAChRs. For the $\alpha6$L9′S mice, low doses of nicotine (0.02–0.15 mg/kg ip) result in locomotor activation ($\sim$350% of saline activity for 0.15 mg/kg nicotine), while in wild type there is no effect of these doses of nicotine, and, in fact, higher doses (0.5–2.0 mg/kg ip) in wild type mice as well as doses over 1 mg/kg in $\alpha6$L9′S mice produce locomotor suppression (Drenan et al., 2008). In addition, the $\alpha6$L9′S-gain-of-function mice have the same temperature depression responses as wild type mice (unpublished data; see Tapper et al., 2007 for wild type), <1 °C temperature decrease with a dose of 0.1 mg/kg nicotine. Thus, this measurement isolates an $\alpha6^*$-nAChR-mediated physiological effect. Representative experiments using Compound 1, identified as a partial agonist at $\alpha4\beta2^*$ and a full agonist at $\alpha6\beta2^*$ in the in vitro assays are shown in Fig. 6. Compound 1 proved active in vivo and stimulated both $\alpha4$L9′A* nAChRs, with 0.03 mg/kg inducing $\sim$8° temperature drop and $\alpha6$L9′S*-nAChRs where 0.01 mg/kg resulted in $\sim$290% increase in activity over saline. Subsequently, the agonists Compounds 2, 8 and 10 were evaluated for their ability to elicit hypothermia or locomotor activation in $\alpha4$L9′A and $\alpha6$L9′S mice. As shown in Table 4, each of these compounds elicited responses in both mutant mice expressing hyperactive nAChR. Compounds 3, 4 and 7, which were identified as antagonists, blocked the effects of 0.1 mg/kg nicotine in vivo. Data for nicotine and varenicline are provided for comparison in Table 4.

4. Discussion

The CNS nAChRs have various roles in normal brain function. These receptors are activated by the natural neurotransmitter, acetylcholine, and their activity may also be modified by the
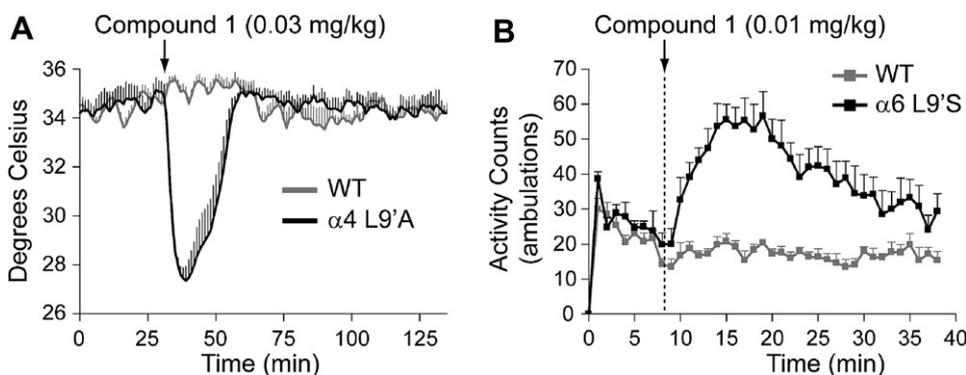
Fig. 6. Physiological assays for hypothermia in α4L9′A mice and locomotor activation in α6L9′S mice by Compound 1. Panel A: Hypothermia measurements in α4L9′A mice to assay Compound 1 bioavailability and *in vivo* activity at α4β2* nAChRs. An averaged (n = 6 mice) whole-body temperature response in α4L9′A and WT control mice in response to an i.p. injection of Compound 1 (0.03 mg/kg) is shown. Panel B: Locomotor activation assay in α6L9′S mice to assess bioavailability and *in vivo* activity at α6β2* nAChRs. Average locomotor activity (n = 8 mice) for α6L9′S and WT control mice is shown in response to an i.p. injection of Compound 1 (0.01 mg/kg). All data shown are means ± sem.

presence of nicotine (Perez et al., 2008). Nicotine from tobacco smoking occupies a large fraction of the α4β2*-nAChR (Brody et al., 2008). Such data are not available for the α6β2*-nAChRs, but if nicotine occupies a lower percentage of these receptors, or desensitizes them less readily, nicotine use could produce an altered balance between GABAergic and dopaminergic function. To better understand the role of the α6β2* and to define the optimal profile for therapeutics targeting nicotine addiction as well as other disorders that are potential targets for nicotinic receptor-based therapy, selective ligands are necessary. The lack of available data around α6β2* SAR and limited structure-function data for other subtypes led us to prepare and/or characterize a number of known and novel ligands across various nicotinic receptor subtypes.

Our data show that commonly studied nicotinic agonists including nicotine, acetylcholine, cytisine and A-85380, bind to α4β2*-nAChR subtype with higher affinity than to α6β2*, and, generally, had lower affinity at both the α7 and α3β4*-subtypes (see Fig. 4A and Table 1). However functional measurements (Fig. 4B and Table 2) reveal that several agonists activate α6β2*-nAChR at lower concentrations than α4β2*-nAChR. Thus, the relationship between binding affinity and functional potency differed markedly between the α6β2*- and α4β2*-nAChRs (see also Salminen et al., 2005). Presumably this disparity arises from inherent differences in relationships among binding, activation and desensitization. Further study will be required to understand this topic. Furthermore the α6β2*-subtype actually comprises several receptors, including α4α6β2β3, which is activated by lower concentrations of nicotine than the α6β3β2 or the α4(non-α6)β2*-nAChR (Salminen et al., 2007).

Table 4
Physiological effects in mice with hypersensitive α4β2* or α6β2*-nAChR.

Compound	α4L9′Aβ2*	α6L9′Sβ2*
Nicotine	hypothermia (0.01)[a]	activation (0.1)[b]
Varenicline	hypothermia (0.001)	activation (0.1)
Compound 1 RJR2429/TC2429	hypothermia (0.03)	activation (0.01)[b]
Compound 2	hypothermia (0.03)	activation (0.1)
Compound 3 TC1698	block (0.002)	
Compound 4	block (0.01)	
Compound 5	no effect	
Compound 6 TC6951		
Compound 7 TC2242	block (0.01)	block (0.1)
Compound 8 RJR2403/TC2403	hypothermia (0.2)	activation (1.0)[b]
Compound 9	no effect	
Compound 10	hypothermia (0.1)	activation (0.1)
Compound 11	inconclusive	

Doses are given as mg/kg.
[a] From Tapper et al. (2007).
[b] From Drenan et al. (2008).

Varenicline (currently marketed as a smoking cessation aid) was also evaluated in our assays. We found that varenicline is a partial agonist at both α4β2* and α6β2*-nAChRs, but a full agonist at both α7 and α3β4* subtypes; these conclusions (for α4β2*, α7 and α3β4* subtypes) agree with data from oocyte-expressed nAChRs (Mihalek et al., 2006) and from rat brain slices (Rollema et al., 2007). Note that the structurally-related compound cytisine, is also a partial agonist at α4β2*-nAChRs (37%); however, cytisine is more efficacious at α6β2* (71%) (Salminen et al., 2004). For varenicline, efficacy is not significantly different between these subtypes for this screen (26 ± 2% and 39 ± 17%, respectively). We found an ∼8-fold ratio of EC_{50} values between α7 and α4β2*-subtypes, the same as previously reported for oocyte-expressed receptors (Mihalek et al., 2006). According to our data in mouse tissue, varenicline is somewhat selective for α4β2*-nAChR when assessed with binding affinity (2-fold over α6β2*, 9-fold over α7 and 24-fold over α3β4*) though considerably less selective than reported for rat brain α4β2* compared to α7 in IMR32 cells (Rollema et al., 2007). Our data on varenicline generally agree with published data from other laboratories (see Supplementary Table 1 for a compilation of data with species, method and source) in finding that it is a partial agonist at α4β2*, with higher efficacy at α7 and α3β4*-nAChR. There may be some species or methods differences in these data.

The structures of a series of nicotine-related compounds that were evaluated in this study are shown in Fig. 1. Within this series, the basic pharmacophoric elements of nicotine (cationic center, hydrogen bond acceptor and aromatic ring) were retained, but elaborated into a set of chemically diverse analogs: 1) the distance from the pyridine to the cationic center is varied, 2) steric bulk of the molecule (particularly the region around the cationic center) is explored, and 3) flexibility is varied from compounds with many degrees of freedom (the meta-nicotines Compounds 8 and 9) to highly constrained (3-pyridinyl-azatricyclo[3.3.1.13,7]decane) Compound 4. Some data on affinity, potency and efficacy have been previously published for certain of these compounds and a comparison of these values, along with species and references, is presented in Supplementary Table 2. As with varenicline, some differences may result from methods or species used. Despite the wide variety of techniques and species, there is considerable agreement where comparable data exist.

The data presented here suggested several observations about the role of structure in affinity and efficacy. Generally, constraining the cationic nitrogen into certain ring variations enhances affinity across all subtypes relative to the open-chain metanicotine. Increasing the conformational constraint further by capturing the cationic center into bicyclic ring systems further enhances affinity. This affinity enhancement is illustrated clearly in the progression from Compound

8 to nicotine to Compound 10 to Compound 3 and finally Compound 1, where the K_i values decrease between one and three orders of magnitude. Binding affinities for the α6β2* and α7 receptors are most affected by these structural changes. (Compound 2 and Compound 4 are excluded from this comparison since they represent more significant changes in pyridine-nitrogen orientation and steric effects, respectively.) It is not clear what factors are responsible for this affinity shift, since these structural changes alter the character of the molecule in several ways. For example, the cationic center is changed from secondary to tertiary, basicity is increased, lone nitrogen electron pair orientation altered, steric bulk is added (which can be both repulsive or provide positive hydrophobic interactions), and bond distances and orientation are all altered. Increasing the distance between the pyridine nitrogen and the cationic nitrogen also appears to greatly reduce affinity across all subtypes. This is qualitatively observed in comparing the properties of nicotine to those of Compound 8, and the properties of Compound 1 to those of structurally related azabicyclics, Compounds 5 and 11.

Comparing efficacy trends within the range of structures examined, here we noted that agonist activity is more readily retained for both the α7 and α3β4*-nAChR subtypes than the α4β2* and α6β2*-nAChR subtypes. This suggests that the binding pockets of the latter subtypes have stricter structural requirements for activation than the former. For example, in the series of Compounds 2, 1, 3 and 4, the azacyclic portion of the molecule is made progressively more sterically demanding. Functional activity at α4β2* shifts to partial agonism and antagonism across the series (43%, 30%, −97%, −100% efficacy compared to nicotine, Fig. 4C and Table 3). Efficacy at the α6β2*-nAChR subtype appears slightly more tolerant of structural modifications to its ligands relative to the α4β2*-nAChR. Here, the decrease in efficacy is more gradual within the series (114%, 109%, −71%, −98%). In contrast, at α7 and α3β4*, these same compounds all retain agonism, with very gradually decreasing efficacy (respective efficacy for α7, 108%, 89%, 106%, 27%; for α3β4*, 118%, 106%, 95%, 88%).

In vitro functional assays for α4β2*- and α6β2*-mediated responses identified the reference compounds, nicotine and varenicline, as full and partial agonists, respectively. Consistent with this identification, both of these compounds induced hypothermia in α4L9′A and locomotor hyperactivity in α6L9′S hypersensitive mice. Likewise, Compounds 1, 2 and 10, identified as full or partial α4β2* and α6β2* agonists *in vitro*, elicited hypothermia and locomotor activation in mice expressing hypersensitive nAChRs (Table 1). Compound 8 with high efficacy at α4β2* also induced hypothermia in α4L9′A mice. Though this compound displayed no measurable activity at α6β2*-nAChR in WT mice *in vitro*, it did elicit a response in α6L9′S mice, consistent with its agonist activity *in vitro* in tissue from these mutant mice (Drenan et al., 2008). Compounds 3, 4 and 7, which were identified *in vitro* as α4β2* and α6β2* antagonists, blocked the effects of nicotine *in vivo*, supporting the premise that they are, indeed, bioavailable antagonists. Results with these agonists and antagonists show that they effectively elicit the expected behavior in mice expressing the mutated receptors. However several compounds identified as antagonists *in vitro* (Compounds 5, 9, and 11) did not have intrinsic activity, nor did they block the effect of nicotine at the doses tested. In the absence of data on bioavailability, it is not possible to determine whether the lack of effect was receptor-based or, more likely, due to low concentration in the brain. It should be emphasized that these mice were designed to respond to agonists at doses much lower than the doses required for wild-type mice, so that α4* and α6*-dependent behavioral responses can be studied in the absence of effects on other AChRs. The hypersensitive mutations are located in the M2 transmembrane domain, some 60 Å from the agonist binding site. Thus while the present *in vivo* data serve well for a qualitative assignment of agonist vs. antagonist, the dose dependence *in vivo* is not relevant to the wild type nAChRs. In addition, correlation between the EC_{50} values measured *in vitro* and the effective concentrations *in vivo* cannot be accurately assessed since potential differences in pharmacokinetics, metabolism and distribution leading to different exposures have not been taken into account.

The functional characterization reported here has allowed us to achieve an important goal for this project, namely, the identification of an agonist selective for the α6β2*-receptor. Both Compounds 1 and 2 fulfilled the requirement for functional selectivity for α6β2* over α4β2*, α7 and α3β4* subtypes, although greater binding selectivity might be desirable. Additionally, both compounds exhibited *in vivo* activity consistent with their *in vitro* profiles. Major questions remain in the design of a safe and effective smoking cessation aid. Which natural functions of nicotinic systems must be preserved to avoid unwanted effects? What minimum level of occupancy is effective for a smoking cessation aid? Is a short-acting agent with high occupancy administered frequently better than one with a long half-life and low occupancy? Is it more effective to activate receptors, to desensitize them, or to chaperone them within intracellular compartments (Lester et al., 2009)? Will selectively targeting α6β2*nAChR prove advantageous relative to other individual or multiple subtypes? Availability of relatively selective, bioavailable compounds such as Compound 1 and 2 or compounds designed on the SAR data reported here may enable research to help answer these questions.

Appendix. Supplementary material

Supplementary data associated with this article can be found in the online version at doi:10.1016/j.neuropharm.2010.01.013.

References

Bencherif, M., Lovette, M.E., Fowler, K.W., Arrington, S., Reeves, L., Caldwell, W.S., Lippiello, P.M., 1996. RJR-2403: a nicotinic agonist with CNS selectivity I. In vitro characterization. J. Pharmacol. Exp. Ther. 279, 1413–1421.

Bhatti, B.S., Strachan, J.P., Breining, S.R., Miller, C.H., Tahiri, P., Crooks, P.A., Deo, N., Day, C.S., Caldwell, W.S., 2008. Synthesis of 2-(pyridin-3-yl)-1-azabicyclo[3.2.2] nonane, 2-(pyridin-3-yl)-1-azabicyclo[2.2.2]octane, and 2-(pyridin-3-yl)-1-azabicyclo[3.2.1]octane, a class of potent nicotinic acetylcholine receptor-ligands. J. Org. Chem. 73, 3497−3507.

Brody, A.L., Mandelkern, M.A., Costello, M.R., Abrams, A.L., Scheibal, D., Farahi, J., London, E.D., Olmstead, R.E., Rose, J.E., Mukhin, A.G., 2008. Brain nicotinic acetylcholine receptor occupancy: effect of smoking a denicotinized cigarette. Int. J. Neuropsychopharmacol. 12, 305−316.

Champtiaux, N., Han, Z.Y., Bessis, A., Rossi, F.M., Zoli, M., Marubio, L., McIntosh, J.M., Changeux, J.P., 2002. Distribution and pharmacology of α6-containing nicotinic acetylcholine receptors analyzed with mutant mice. J. Neurosci. 22, 1208−1217.

Champtiaux, N., Gotti, C., Cordero-Erausquin, M., David, D.J., Przybylski, C., Léna, C., Clementi, F., Moretti, M., Rossi, F.M., Le Novère, N., McIntosh, J.M., Gardier, A.M., Changeux, J.P., 2003. Subunit composition of functional nicotinic receptors in dopaminergic neurons investigated with knock-out mice. J. Neurosci. 23, 7820−7829.

Coe, J.W., Brooks, P.R., Vetelino, M.G., Wirtz, M.C., Arnold, E.P., Huang, J., Sands, S.B., Davis, T.I., Lebel, L.A., Fox, C.B., Shrikhande, A., Heym, J.H., Schaeffer, E.,

Rollema, H., Lu, Y., Mansbach, R.S., Chambers, L.K., Rovetti, C.C., Schulz, D.W., Tingley 3rd, F.D., O'Neill, B.T., 2005. Varenicline: an α4β2 nicotinic receptor partial agonist for smoking cessation. J. Med. Chem. 48, 3474–3477.

De Biasi, M., Salas, R., 2008. Influence of neuronal nicotinic receptors over nicotine addiction and withdrawal. Exp. Biol. Med. (Maywood) 233, 917–929.

Drenan, R.M., Grady, S.R., Whiteaker, P., McClure-Begley, T., McKinney, S., Miwa, J.M., Bupp, S., Heintz, N., McIntosh, J.M., Bencherif, M., Marks, M.J., Lester, H.A., 2008. In vivo activation of midbrain dopamine neurns via sensitized, high-affinity α6 nicotinic acetylcholine receptors. Neuron 60, 123–136.

Dunlop, J., Roncarati, R., Jow, B., Bothman, H., Lock, T., Kowal, D., Bowlby, M., Terstappen, G.C., 2007. In vitro screening strategies for nicotinic receptor ligands. Biochem. Pharmacol. 74, 1172–1181.

Exley, R., Clements, M.A., Hartung, H., McIntosh, J.M., Cragg, S.J., 2008. α6-containing nicotinic acetylcholine receptors dominate the nicotine control of dopamine neurotransmission in nucleus accumbens. Neuropsychopharmacology 33, 2158–2166.

Flores, C.M., Rogers, S.W., Pabreza, L.A., Wolfe, B.B., Kellar, K.J., 1992. A subtype of nicotinic cholinergic receptor in rat brain is composed of α4 and β2 subunits and is up-regulated by chronic nicotine treatment. Mol. Pharmacol. 41, 31–37.

Gohlke, H., Schwarz, S., Guendisch, D., Tilotta, M.C., Weber, A., Wegge, T., Seitz, G., 2003. 3D QSAR analyses-guided rational design of novel ligands for the $(\alpha 4)_2 (\beta 2)_3$ nicotinic acetylcholine receptor. J. Med. Chem. 46, 2031–2048.

Gotti, C., Zoli, M., Clementi, F., 2006. Brain nicotinic acetylcholine receptors: native subtypes and their relevance. Trends Pharmacol. Sci. 27, 482–491.

Grady, S.R., Meinerz, N.M., Cao, J., Reynolds, A.M., Picciotto, M.R., Changeux, J.P., McIntosh, J.M., Marks, M.J., Collins, A.C., 2001. Nicotinic agonists stimulate acetylcholine release from mouse interpeduncular nucleus: a function mediated by a different nAChR than dopamine release from striatum. J. Neurochem. 76, 258–268.

Ho, M.K., Tyndale, R.F., 2007. Overview of the pharmacogenomics of cigarette smoking. Pharmacogenomics J. 7, 81–98.

Hoft, N.R., Corley, R.P., McQueen, M.B., Schlaepfer, I.R., Huizinga, D., Ehringer, M.A., 2008. Genetic association of the CHRNA6 and CHRNB3 genes with tobacco dependence in a Nationally representative sample. Neuropsychopharmacology 34, 698–706.

Keath, J.R., Iacoviello, M.P., Barrett, L.E., Mansvelder, H.D., McGehee, D.S., 2007. Differential modulation by nicotine of substantia nigra versus ventral tegmental area dopamine neurons. J. Neurophysiol. 98, 3388–3396.

Lai, A., Parameswaran, N., Khwaja, M., Whiteaker, P., Lindstrom, J.M., Fan, H., McIntosh, J.M., Grady, S.R., Quik, M., 2005. Long-term nicotine treatment decreases striatal α6* nicotinic acetylcholine receptor sites and function in mice. Mol. Pharmacol. 67, 1639–1647.

Lerman, C., LeSage, M.G., Perkins, K.A., O'Malley, S.S., Siegel, S.J., Benowitz, N.L., Corrigall, W.A., 2007. Translational research in medication development for nicotine dependence. Nat. Rev. Drug Discov. 6, 746–762.

Lester, H.A., Xiao, C., Srinivasan, R., Son, C.D., Miwa, J., Pantoja, R., Banghart, M.R., Dougherty, D.A., Goate, A.M., Wang, J.C., 2009. Nicotine is a selective pharmacological chaperone of acetylcholine receptor number and stoichiometry. Implications for drug discovery. AAPS J. 11, 167–177.

Mameli-Engvall, M., Evrard, A., Pons, S., Maskos, U., Svensson, T.H., Changeux, J.P., Faure, P., 2006. Hierarchical control of dopamine neuron-firing patterns by nicotinic receptors. Neuron 50, 911–921.

Marks, M.J., Stitzel, J.A., Romm, E., Wehner, J.M., Collins, A.C., 1986. Nicotine binding sites in rat and mouse brain: comparison of acetylcholine, nicotine and α-bungarotoxin. Mol. Pharmacol. 30, 427–436.

Marks, M.J., Farnham, D.A., Grady, S.R., Collins, A.C., 1993. Nicotinic receptor function determined by stimulation of rubidium efflux from mouse brain synaptosomes. J. Pharmacol. Exp. Ther. 264, 542–552.

Marks, M.J., Smith, K.W., Collins, A.C., 1998. Differential agonist inhibition identifies multiple epibatidine binding sites in mouse brain. J. Pharmacol. Exp. Ther. 285, 377–386.

Marks, M.J., Whiteaker, P., Calcaterra, J., Stitzel, J.A., Bullock, A.E., Grady, S.R., Picciotto, M.R., Changeux, J.P., Collins, A.C., 1999. Two pharmacologically distinct components of nicotinic receptor-mediated rubidium efflux in mouse brain require the β2 subunit. J. Pharmacol. Exp. Ther. 289, 1090–1103.

Marks, M.J., Whiteaker, P., Collins, A.C., 2006. Deletion of the α7, β2, or β4 nicotinic receptor subunit genes identifies highly expressed subtypes with relatively low affinity for [^{3}H]epibatidine. Mol. Pharmacol. 70, 947–959.

Marks, M.J., Meinerz, N.M., Drago, J., Collins, A.C., 2007. Gene targeting demonstrates that α4 nicotinic acetylcholine receptor subunits contribute to expression of diverse [^{3}H]epibatidine binding sites and components of biphasic ^{86}Rb$^+$ efflux with high and low sensitivity to stimulation by acetylcholine. Neuropharmacology 53, 390–405.

McCallum, S.E., Collins, A.C., Paylor, R., Marks, M.J., 2006. Deletion of the β2 nicotinic acetylcholine receptor subunit alters development of tolerance to nicotine and eliminates receptor upregulation. Psychopharmacol. (Berl.) 184, 314–327.

Mihalek, K.B., Carroll, F.I., Luetje, C.W., 2006. Varenicline is a partial agonist at α4β2 and a full agonist at α7 neuronal nicotinic receptors. Mol. Pharmacol. 70, 801–805.

Nashmi, R., Xiao, C., Deshpande, P., McKinney, S., Grady, S.R., Whiteaker, P., Huang, Q., McClure-Begley, T., Lindstrom, J.M., Labarca, C., Collins, A.C., Marks, M.J., Lester, H.A., 2007. Chronic nicotine cell specifically upregulates functional α4* nicotinic receptors: basis for both tolerance in midbrain and enhanced long-term potentiation in perforant path. J. Neurosci. 27, 8202–8218.

Perez, X.A., Bordia, T., McIntosh, J.M., Grady, S.R., Quik, M., 2008. Long-term nicotine treatment differentially regulates striatal α6α4β2* and α6(non-α4)β2* nAChR expression and function. Mol. Pharmacol. 74, 844–853.

Perry, D.C., Mao, D., Gold, A.B., McIntosh, J.M., Pezzullo, J.C., Kellar, K.J., 2007. Chronic nicotine differentially regulates α6- and β3-containing nicotinic cholinergic receptors in rat brain. J. Pharmacol. Exp. Ther. 322, 306–315.

Pons, S., Fattore, L., Cossu, G., Tolu, S., Porcu, E., McIntosh, J.M., Changeux, J.P., Maskos, U., Fratta, W., 2008. Crucial role of α4 and α6 nicotinic acetylcholine receptor subunits from ventral tegmental area in systemic nicotine self-administration. J. Neurosci. 28, 12318–12327.

Quik, M., Sum, J.D., Whiteaker, P., McCallum, S.E., Marks, M.J., Musachio, J., McIntosh, J.M., Collins, A.C., Grady, S.R., 2003. Differential declines in striatal nicotinic receptor subtype function after nigrostriatal damage in mice. Mol. Pharmacol. 63, 1169–1179.

Rollema, H., Chambers, L.K., Coe, J.W., Glowa, J., Hurst, R.S., Lebel, L.A., Lu, Y., Mansbach, R.S., Mather, R.J., Rovetti, C.C., Sands, S.B., Schaeffer, E., Schultz, D.W., Tingley III, F.D., Williams, K.E., 2007. Pharmacological profile of the α4β2 nicotinic acetylcholine receptor partial agonist varenicline, an effective smoking cessation aid. Neuropharmacology 52, 985–994.

Salminen, O., Murphy, K.L., McIntosh, J.M., Drago, J., Marks, M.J., Collins, A.C., Grady, S.R., 2004. Subunit composition and pharmacology of two classes of striatal presynaptic nicotinic acetylcholine receptors mediating dopamine release in mice. Mol. Pharmacol. 65, 1526–1535.

Salminen, O., Whiteaker, P., Grady, S.R., Collins, A.C., McIntosh, J.M., Marks, M.J., 2005. The subunit composition and pharmacology of α-Conotoxin MII-binding nicotinic acetylcholine receptors studied by a novel membrane-binding assay. Neuropharmacology 48, 696–705.

Salminen, O., Drapeau, J.A., McIntosh, J.M., Collins, A.C., Marks, M.J., Grady, S.R., 2007. Pharmacology of α-conotoxin MII-sensitive subtypes of nicotinic acetylcholine receptors isolated by breeding of null mutant mice. Mol. Pharmacol. 71, 1563–1571.

Tapper, A.R., McKinney, S.L., Marks, M.J., Lester, H.A., 2007. Nicotine responses in hypersensitive and knockout α4 mice account for tolerance to both hypothermia and locomotor suppression in wild-type mice. Physiol. Genomics 31, 422–428.

Tumkosit, P., Kuryatov, A., Luo, J., Lindstrom, J., 2006. β3 subunits promote expression and nicotine-induced up-regulation of human nicotinic α6* nicotinic acetylcholine receptors expressed in transfected cell lines. Mol. Pharmacol. 70, 1358–1368.

Whiteaker, P., Jimenez, M., McIntosh, J.M., Collins, A.C., Marks, M.J., 2000a. Identification of a novel nicotinic binding site in mouse brain using [^{125}I]-epibatidine. Br. J. Pharmacol. 131, 729–739.

Whiteaker, P., McIntosh, J.M., Luo, S., Collins, A.C., Marks, M.J., 2000b. ^{125}I-α-conotoxin MII identifies a novel nicotinic acetylcholine receptor population in mouse brain. Mol. Pharmacol. 57, 913–925.

Whiteaker, P., Peterson, C.G., Xu, W., McIntosh, J.M., Paylor, R., Beaudet, A.L., Collins, A.C., Marks, M.J., 2002. Involvement of the α3 subunit in central nicotinic binding populations. J. Neurosci. 22, 2522–2529.

Zeiger, J., Haberstick, B.C., Schlaepfer, I., Collins, A.C., Corley, R.P., Crowley, T.J., Hewitt, J.K., Hopfer, C.J., Lessem, J., McQueen, M.B., Rhee, S.H., Ehringer, M.A., 2008. The neuronal nicotinic receptor subunit genes (CHRNA6 and CHRNB3) are associated with subjective responses to tobacco. Hum. Mol. Genet. 17, 724–734.

Zhao, Chunlin, Zhang, Min, Gabriel, Jerome L., Caldwell, William S., Bencherif, Merouane, Canney, Daniel J., 2002, Structure-activity Relationship Study of 2- and 3-substituted Quinuclidines as Ligands for Cholinergic Receptors, Abstracts of Papers, 223rd ACS National Meeting, Orlando, FL, United States, April 7–11, MEDI-040.